Bulletin of the Seismological Society of America, Vol. 92, No. 3, pp. 983–997, April 2002

Recent Rupture History of the San Andreas Fault Southeast of Cholame in the Northern Carrizo Plain, California

by Elizabeth M. Stone, Lisa B. Grant, and J Ramón Arrowsmith

Abstract We conducted a paleoseismic study on the San Andreas fault (SAF) southeast of Cholame, California, to investigate the record of earthquakes along an 80-km paleoseismic data gap between Parkfield and the Carrizo Plain. At the LY4 site, located 37.5 km southeast of Highway 46 along the SAF, we excavated a fault-perpendicular trench on the distal end of an alluvial fan that emanates from the Temblor Mountains to the northeast. We found evidence of three and possibly four ruptures recorded within the stratigraphy. The only age constraints are radiocarbon dates on a paleosol three units (50 cm) below the oldest event horizon and the presence of recently introduced exotic pollen species in an upper unit. The radiocarbon dates indicate there have been at least three surface-rupturing events at the LY4 site since cal. A.D. 1058–1291. Exotic (historic) pollen in the top of a unit possibly cut by the youngest event suggests that an earthquake affected at the LY4 site close to A.D. 1873–1874.

Introduction

The Cholame segment of the San Andreas fault (SAF) stretches between Highway 46 at Cholame and Highway 58 in the northern Carrizo Plain (Fig. 1) (Working Group on California Earthquake Probabilities [WGCEP] 1988). The northern segment boundary is defined by the location where the fault behavior changes from partially creeping in the north to locked in the south. This location has also been the southern termination of recent Parkfield ruptures (Bakun and Lindh, 1985; Bakun and Wentworth, 1997). The southern segment boundary is defined by the increase in the magnitude of geomorphic offsets attributed to the 1857 earthquake in the Carrizo Plain, as mapped by Sieh (1978b). Several attempts to characterize the earthquake potential of the Cholame segment have emphasized the need for better paleoseismic data (WGCEP, 1988; Southern California Earthquake Center Working Group [SCECWG], 1994; Arrowsmith *et al.*, 1997). In addition, paleoseismic studies in the Carrizo Plain have raised questions about recurrence models that can be better tested if data are obtained for the Cholame segment (Sieh and Jahns, 1984; Grant and Sieh, 1994; Grant, 1996). Our data address unresolved questions related to the rupture potential and past behavior of the San Andreas fault in this area.

Because there is no published paleoseismic record from the Cholame segment, the only data available to interpret models for earthquake history and rupture potential are the offset geomorphic features along this section of the fault. However, geomorphic offsets are inherently ambiguous, and those along the Cholame segment have been debated; they have been interpreted to average either 3–4 m (Sieh, 1978b) or 6 m (Lienkaemper and Sturm, 1989; Lienkaemper, 2002). These differences are significant when used to estimate earthquake recurrence. Paleoseismic data can provide recent earthquake recurrence information and constrain the recurrence intervals that, previous to this study, were based largely on measurement of offset geomorphic features.

In this article, we present the results of a paleoseismic study along the Cholame segment. We mapped and trenched the LY4 site, shown in Figures 1–3. We have interpreted the occurrence of three and possibly four surface-faulting events in the stratigraphy of this trench. Because of the paucity of datable material, we were unable to resolve the dates of individual events, but we do calculate an average recurrence interval and place some constraints on the date of the most recent surface rupture.

LY4 Site Description and Challenges

The natural environment and human activities in the Cholame–Carrizo area pose challenges to successful completion of paleoseismic investigations. This is one of the reasons for the sparse paleoseismic data in this region. Paleoseismic sites must be chosen carefully to identify a location that preserves distinct evidence of multiple ruptures. There are four important considerations for choosing a paleoseismic site: (1) frequent deposition of bedded sediments, (2) production and preservation of datable material, (3) a well-defined fault trace, and (4) a well-located fault trace. Sedimentation must be frequent enough so that multiple lay-

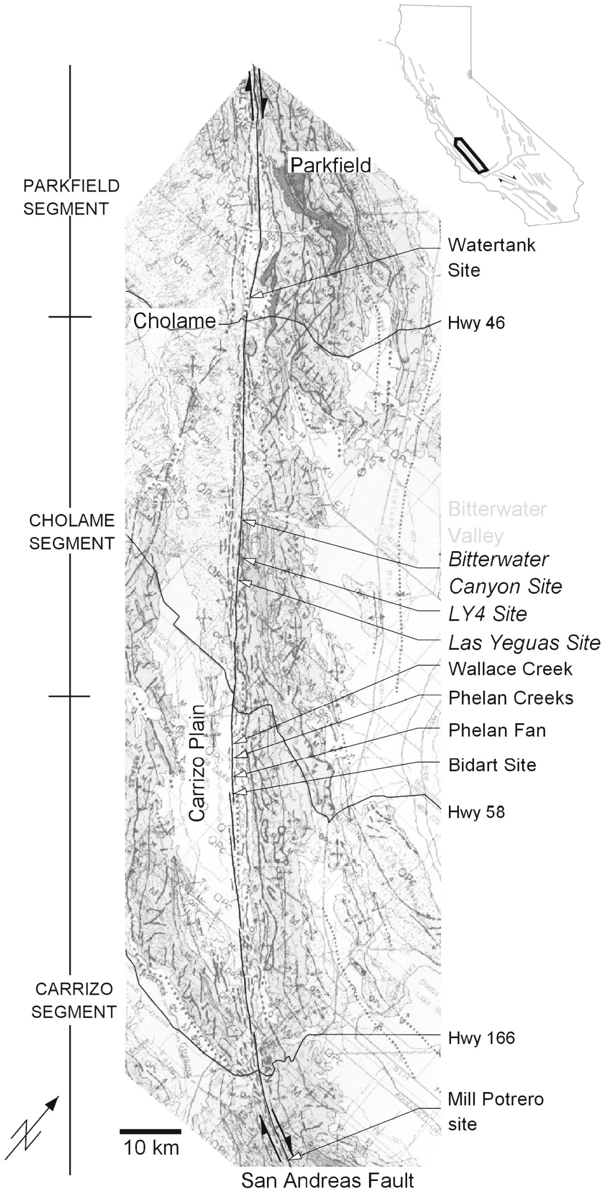

Figure 1. Important sites along the Parkfield, Cholame, and Carrizo segments of the SAF. The northern boundary of the Cholame segment is at Highway 46, and the southern boundary is at Highway 58. The distance between existing paleoseismic sites in the Carrizo Plain and the Watertank site of Sims (1987) is 73 km. The Las Yeguas and Bitterwater Canyon sites are described by Stone (1999). We excavated at the LY4 site. The background is from the 1:750,000 scale state geologic map (Jennings *et al.*, 1977), and the inset in the upper right shows the major faults of California and the extent of the figure. Modified from Arrowsmith *et al.* (1997).

ers will be deposited between surface-rupturing events. Frequent sedimentation also minimizes stratigraphic disruption by burrowing animals. However, if the rate of sedimentation is too high, the event horizons will be too far apart and only one or two events can be seen in a standard (4 m deep) trench. Finally, one of the most important aspects of paleoseismic work is dating ruptures, which requires precisely datable material such as charcoal or peat layers.

It has been difficult to find a site on the Cholame segment that meets these criteria. There are virtually no peat-forming locations or depositional settings that reliably preserve datable charcoal. Additional complications are caused by recently (within the past ~150 yr) altered erosion and deposition rates and patterns. This has been observed throughout the southwest and is interpreted to be a result of either cattle ranching (which became common within this area during the 1850s) or a climatic change around the same time, or a combination of the two (Graf, 1988). Many of the incised drainages that cross the fault are not offset because the incision is younger than the 1857 earthquake. Some alluvial fans that have been reactivated by grazing contain a massive subsurface layer, indicating an older bioturbated surface, which is covered by post-1850s sediment. The southern end of the Cholame segment also has a rift valley geomorphic expression. Much of the drainage is parallel to the fault, in contrast to the relatively simple geomorphology and perpendicular flow of the northern Cholame segment and the Carrizo Plain farther to the south (e.g., Wallace Creek). In addition, most of the land along the Cholame segment is privately owned by ranchers who are reluctant to allow access to researchers.

We identified the LY4 site after extensive mapping, site evaluation, and landowner negotiations along the southeastern half of the Cholame segment of the SAF (see Stone [1999] for map data and description of alternate but inaccessible sites). The LY4 trench site is located on the middle of three alluvial fans derived from subparallel drainages from the Temblor Range (Figs. 2, 3a) to the northeast. The fans have been deposited on a surface cut by a stream that drains to the northwest parallel to the fault. The northwest fan (shown as NW fan in Fig. 3) may have been modified either during road construction or gypsum prospecting and therefore was not deemed suitable for further work. The southeast fan terminates against a scarp, and deposits do not appear to cross the fault. The middle fan is most suitable for paleoseismic investigation because the fault trace crosses the distal end of the fan, where sedimentation would occur almost as frequently as the rest of the fan, but the sedimentation rates would be lower and the sediment would be finer grained (Fig. 3). The fan terminates against a fluvially degraded hill (later buried by the alluvial sediments), which blocked the flow of water and caused local ponding of sediments and water. Ponding no longer occurs because there is now incision on the southwest side of the hill (Fig. 3).

The fault geometry in the area of the LY4 site is well expressed and geomorphically simple (Figs. 2 and 3). There is a steep (~6 m high) 100-m-long fault scarp approximately 100 m southeast of the LY4 trench site, and 150 m beyond that is a saddle where the fault cuts a sliver off an old fault or fluvial scarp (Stone, 1999). The fault strand to the northwest of the site is less pronounced. More than one strand

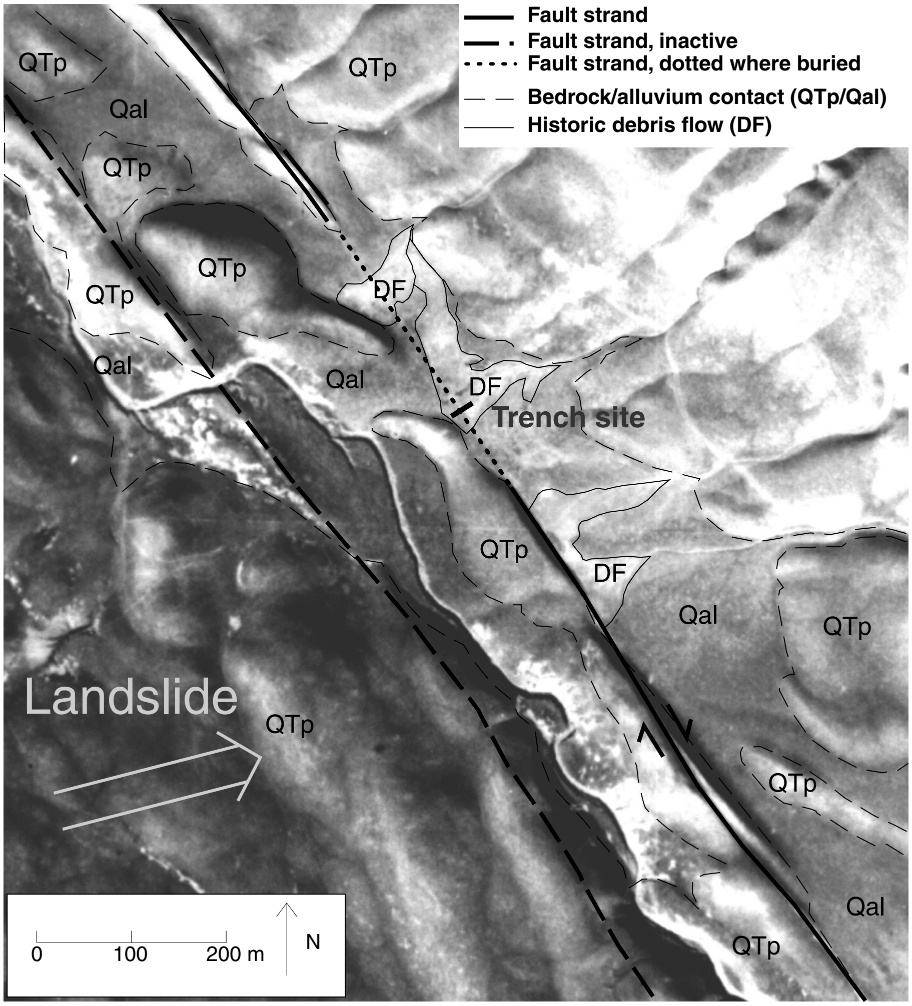

Figure 2. Aerial photo of the LY4 site. Drainages from the Temblor Range to the northeast deposit sediments in alluvial fans that cross the fault. Qal, Quaternary alluvium; QTp, Quaternary–Late Tertiary Paso Robles Formation (Dibblee, 1973); DF, debris flow. Fault strands are dashed where poorly expressed or inactive. See text for description of the site. Aerial photographs are presented courtesy of the Fairchild Aerial Photography collection at Whittier College, Flight C-1260, taken in December 1930.

may be present on the northeast and southwest sides of the hill defining the fault trace (Fig. 3). There is another fault trace 200 m southwest of the fault trace at the LY4 site (Stone, 1999). Our interpretation of geomorphic evidence implies that the southwest strand has not been active recently or has a low slip rate for the last few ruptures (Fig. 2) because expression of this second strand is not as sharp as the strand at the LY4 site. Furthermore, the surface expression of the strand appears to have been displaced by a large landslide on the southwest side of the rift valley. The southeast end of this older scarp is curvilinear and coincides with the concentric ridges of the slide suggesting that as the slide moved to the northeast, it displaced the surface trace of the fault. Between the slide ridges are deposits that exhibit well-developed, hummocky ground patterns and mounds. Wallace (1991) studied the effect of ground squirrels on surfaces in the Carrizo Plain and found that patterned ground formed by burrowing animals can provide an estimate of surface age. More recent mapping and excavations in the Carrizo Plain and Cholame region confirm that mounds and patterned ground are generally correlated with soil development and age of surfaces (Grant, 1993; Stone, 1999). For example, most of the surfaces near the LY4 site are smooth and therefore younger. The presence of patterned ground and mounds between the landslide ridges indicates that the deposits have probably been stable for hundreds of years and perhaps as long as several thousand years, implying that the landslide has not been recently active. Because there are no new scarps in this area, we suspect that the southwest fault strand has not been recently active although we cannot rule out a relatively small amount of displacement in the last few earthquakes.

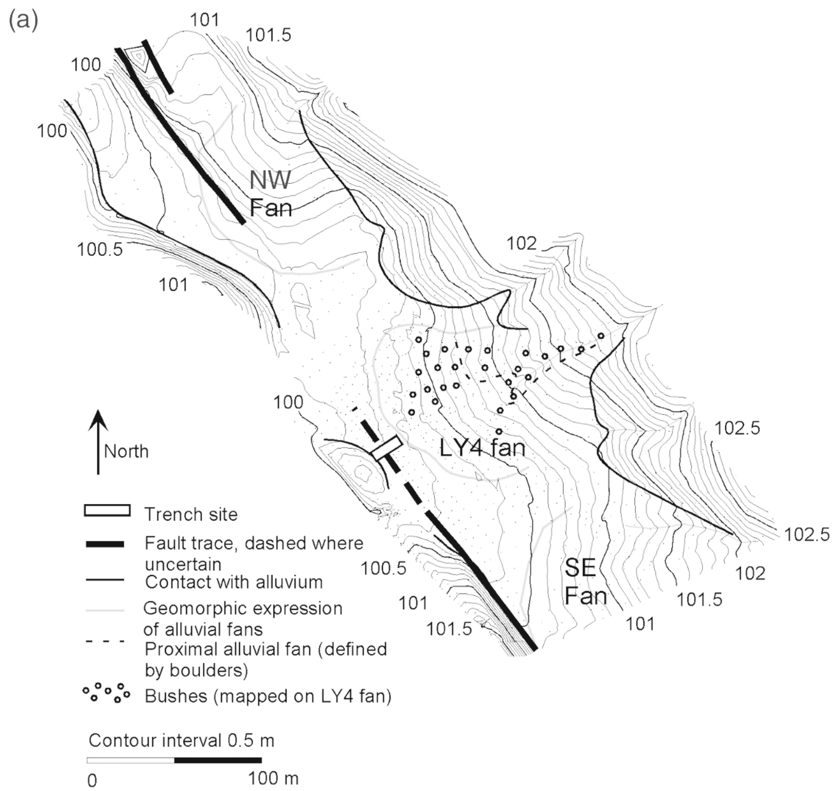

Figure 3. (a) Topographic map of the LY4 site. On the LY4 fan, the fault trace is buried by the distal sediments deposited beyond the geomorphic expression of the fan. In the past, ponding likely occurred at the distal end of the fan, but currently two small drainages about 30 m south of the trench site allow an outlet for water. To the northwest and southeast of the trench site, the fault trace is defined by steep slopes. Contour interval is 0.5 m. Elevations are relative to an arbitrary datum. (b) Photo looking southeast toward the trench site (excavated immediately in front of the trucks) from the northwest end of map shown in Figure 3a (NW). Just beyond the site is a steep scarp and beyond that a saddle that defines the fault trace. A subtle change in soil color on the hill in the foreground defines the main trace.

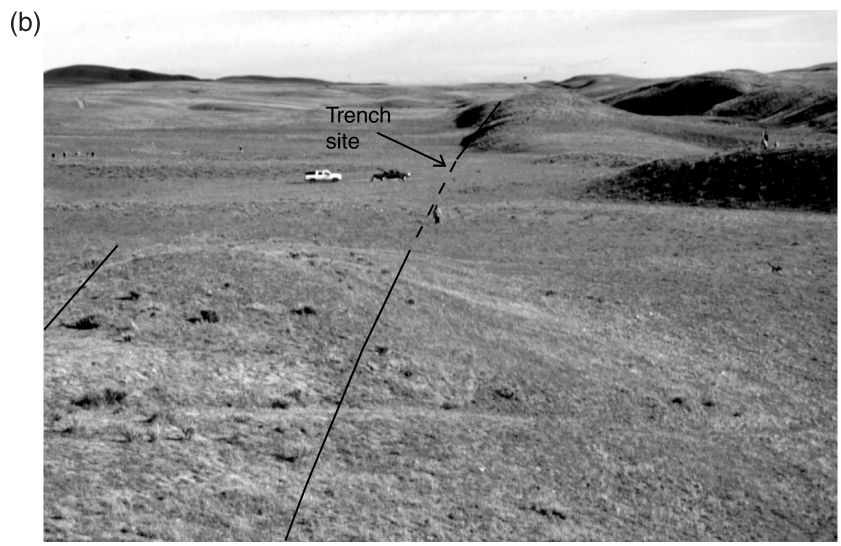

Fault Zone Stratigraphy

A 20-m-long by ~3-m-deep trench was excavated across and perpendicular to the fault trace. We flagged contacts, fractures, sample locations, and other important features with nails and surveyed them with a total station. These data were converted from the northing–easting coordinate system to distance along trench and depth. Both trench walls were mapped on plots of these control points at 1:10 scale. The numbering scheme for the units starts at the bottom with the lowest number, and the major units were numbered in increments of five. Earthquake event horizons are labeled so higher numbers indicate older events.

The stratigraphy of the LY4 site is summarized in Figure 4, and logs of both trench walls are shown on Figures 5 and 6. The stratigraphy northeast and southwest of the fault is significantly different. Three meters of layered alluvial deposits that have experienced only minor amounts of bioturbation are present on the northeast (downthrown) side of the fault. These deposits include silt, sand, and gravel beds, as well as some weakly formed paleosols, and slightly indurated sand, silt, and clay deposits near the bottom of the

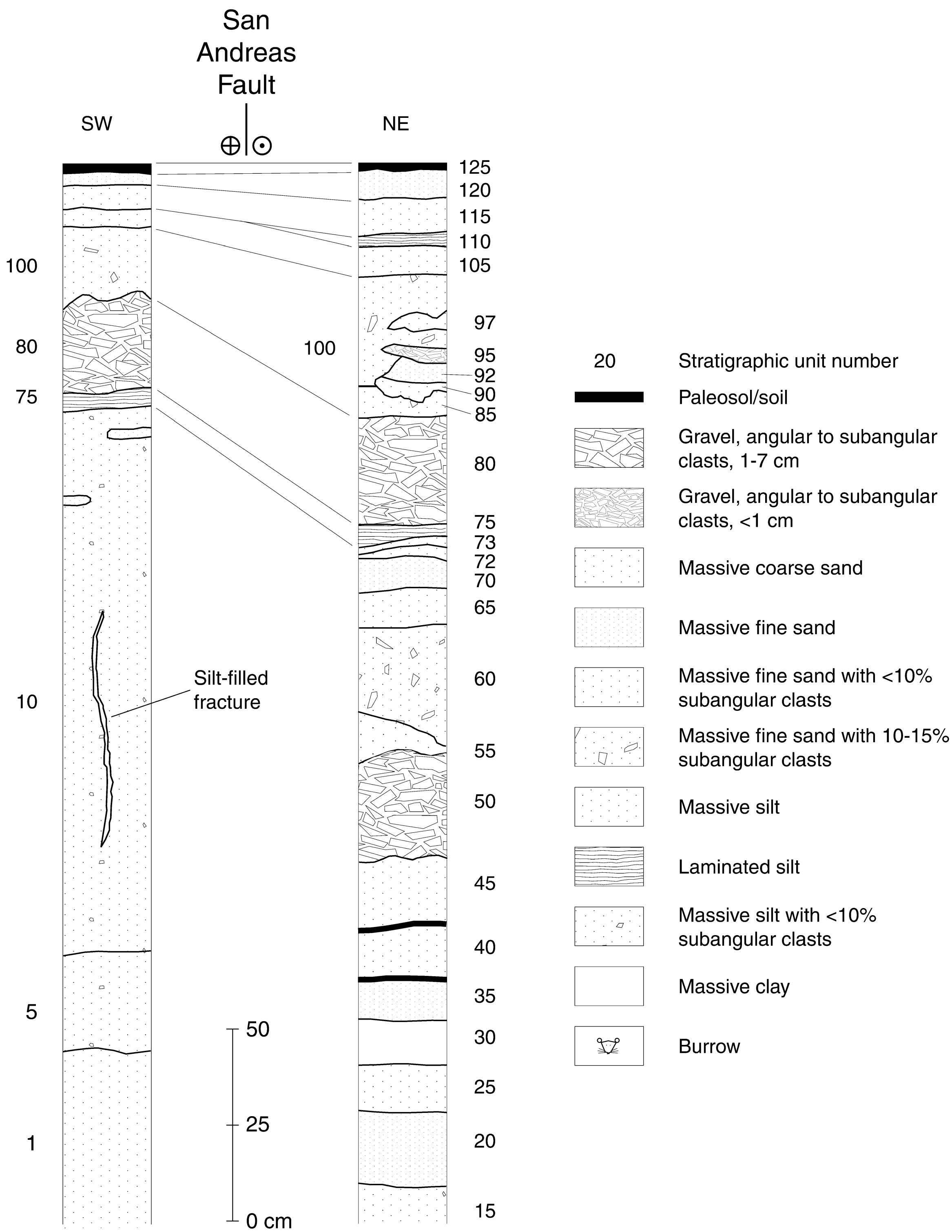

Figure 4. Stratigraphic column of the sediments at the LY4 site. There is a notable lack of stratigraphy southwest of the fault zone except for the upper meter. This suggests that unit 10 was previously exposed and bioturbated. Unit 10 is a continuation of the hill southwest of the trench site (Figs. 2 and 3a). Northeast of the fault zone, there is little bioturbation in a continuous sequence of alluvial sediments. A significant mismatch in stratigraphy across the fault below unit 75 indicates that the units below 75 on the northeast side were either deposited against a scarp or were offset by subsequent faulting.

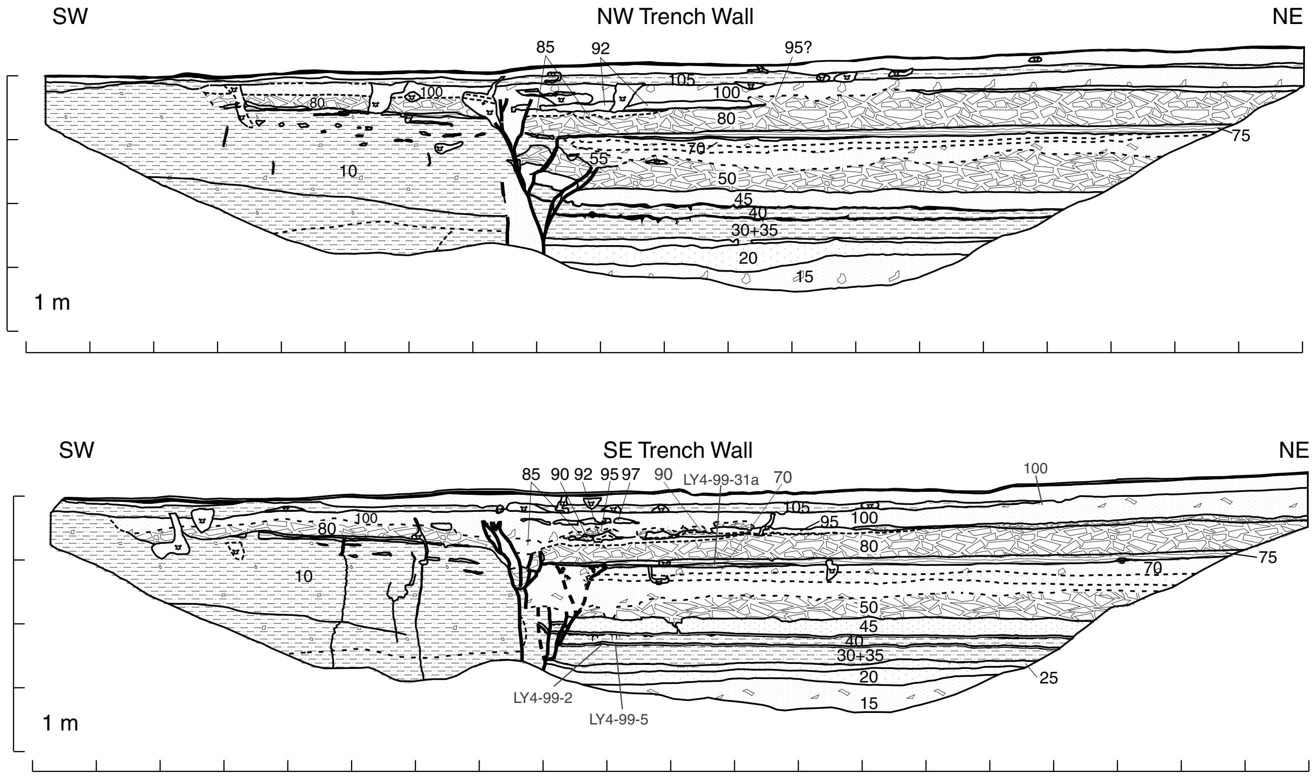

Figure 5. Log of trench walls at the LY4 site. Fault strands cutting and buried by the stratigraphy provide evidence for up to four events, two with apparent vertical offset, and two without vertical offset. Multiple evidence for each rupture is limited because of the narrow fault-zone width. Unit 10 contained fissures filled with vertically laminated silt, which we interpreted as fault strands, but although these strands increase the actual width of the fault zone, they do not provide any information on earthquake ages. See Figure 6 for enlarged views of the fault zone. Logging was originally completed at 1:10 scale. Spatial control comes from total station survey of marker features. The patterns are the same as those in Figure 4. Radiocarbon sample locations and locations of bulk sediment used in pollen analysis for units 70, 90, and 100 are indicated by gray labels (see Tables 1 and 2).

trench. Some of the younger units are derived from the northeast (units 75–125) and cross the fault, but many of the older units are not. The majority of the stratigraphy southwest of the fault is composed of a 1.5-m-thick indurated silt interspersed with a small amount of gravel (unit 10). There are remnants of bedding within unit 10 (note discontinuous layering in upper meter, Fig. 5), but most of the layering has been disrupted, presumably by bioturbation. Also present in this unit are vertically laminated silt-filled fractures that we interpret as rupture strands. This stratigraphy closely matches our expectations based on the local geomorphology of an alluvial fan depositing sediment and burying a small hillslope to the southwest.

The units northeast of the main fault zone provide a good stratigraphic record of fault rupture history because the layering is well defined. The fault zone as seen in the excavation is narrow ($\sim$2 m wide, as opposed to other excavations, such as by Grant and Sieh (1994), in which the fault zone was 12–20 m wide) and extends no more than 1.5 m northeast of the major mismatch in stratigraphy (Fig. 5). Our interpretation of the rupture history at the LY4 site is based entirely on faulting within these units. The lower third of the trench northeast of the fault zone contains indurated units of well-sorted sand, silt, and clay (units 15–45). Two of these units (35 and 40) are capped by dark, 10- to 20-cm thick paleosols (A horizons) that contain abundant small fragments of detrital charcoal. The upper two-thirds of the northeast portion of the trench is characterized by units that are not indurated and are generally not as well sorted (units 50–125). These layers contain matrix-supported debris flow deposits, gravel, sand, and silt. If there is a significant erosional unconformity in the trench, it is likely to be between units 45 and 50. The contact would have to be erosional because there is little evidence for bioturbation and paleosol formation in unit 45. (For example, Grant and Sieh [1994] reported that recognizable paleosols formed within a few decades after deposition of comparable sedimentary units in the Carrizo Plain.) The lower units have gypsum filaments and are more indurated. These differences could also be attributed to groundwater flow and sorting that has contributed to the character of the lower units, and not to a significant difference in age.

In contrast to the units northeast of the fault, unit 10 (Fig. 5) is not useful for interpreting rupture history. Unit 10 is interpreted to be partly colluvial slope wash and partly a continuation of the nearby hillslope to the southwest of the fault (see Fig. 3). This unit also developed many surficial drying cracks on the trench wall shortly after the trench was opened. These cracks were difficult to distinguish from faults. Only those fractures that had been filled with vertically laminated silt were suspected to be faults because they must have been present before the trench was opened. These potential fault strands were not helpful for interpreting rupture history, but they suggest that the total width of the fault zone is at least 4.2 m, greater than the 2 m of major disruption seen in the northeast units (Fig. 5).

There are few units that cross the entire fault zone. The youngest units (units 105, 115, 120, and 125) all cross the fault and exhibit no evidence of rupture. Immediately below them is unit 100, a massive, poorly sorted bed with matrix-supported gravel. We interpret unit 100 as a debris flow deposit with sparse to significant disruption by bioturbation. The amount of bioturbation is difficult to determine but is important for interpeting the number of events, as described subsequently. Unit 100 is present on both sides of the fault. It is the stratigraphically highest unit that exhibits evidence of faulting. Units 80 and 75 are the oldest units that cross the entire fault zone. Unit 75 and the base of unit 80 exhibit apparent vertical displacement of approximately 0.4 m across the fault zone. Several observations suggest that unit 80 was deposited in an alluvial channel: large clasts, sharp (scoured) lower contact, and different elevations of the lower contact on opposite walls of the trench on the same side of the fault (Fig. 5). The elevation difference may reflect the local channel gradient.

Unit 100 directly overlies unit 80 on the southwest side of the fault. On the northeast side, units 85 through 95 are between unit 80 and the top of unit 100. Unit 85 extends into the fault zone but does not cross the fault. Unit 95 is identified only on the southeast wall of the trench. Unit 95 may be present and unrecognized on the other wall because it is texturally similar to unit 80 beneath it. Unit 97 is a discontinuous, irregularly shaped and bioturbated silt layer that appears to be within unit 100. We interpret unit 97 as an abandoned burrow that was filled with silt and then partially reoccupied.

There are three possible explanations for the formation and distribution of units 85–95. The first hypothesis is that they were deposited against an uphill-facing scarp formed by earlier faulting of unit 80. In this scenario, units 85–95 are younger than unit 80 and were deposited after a faulting event (event C2 described subsequently). Unit 80 is significantly thinner on the southwest (upthrown) side of the fault, suggesting that the upper part of unit 80 was eroded after faulting and prior to deposition of unit 100. A second explanation is that units 90–95 are anastomosing beds in the upper part of channel deposits that consist primarily of unit 85. In this hypothesis, units 85–95 could have been deposited at the same time as unit 80, or afterward. Since they do not cross the fault zone, their age relative to the faulting events is not clear. A third hypothesis is that units 90–95 and 97 represent facies changes within unit 100 or remnants of stratigraphy that was destroyed by bioturbation elsewhere within unit 100. Unit 100 appears to have less organic component and clay than other bioturbated sections of the trench. However, unit 100 is poorly sorted, generally massive, and present on both sides of the fault zone and both walls of the trench. It is difficult to explain why an otherwise massive debris flow would exhibit significant local facies changes unless the unit is bioturbated.

Within the fault zones, it is possible to correlate some of the stratigraphy with units outside the fault zone. On the northwest wall of the trench, units 35, 40, 45, and 50 are present within the fault zone. On the southeast wall, it was possible to identify units 35, 40, 45, 75, 80, and 85 within the fault zone. Other units within the fault zones are either sheared or featureless and poorly sorted. These units cannot be identified with confidence.

Paleoseismic Events

The geologic relations at the LY4 site suggest that there have been at least three, and possibly four, ground-rupturing earthquakes during the age of the stratigraphic sequence exposed in the trench (Fig. 5). From oldest to youngest, the event horizons defining the ground surface at the time of each earthquake are interpreted to be the top of units 50, 70, and 80–95, or 100. The oldest event, C4, caused apparent vertical offset that is not present above unit 50 (Fig. 6a). The C3 event horizon is based on fracturing that truncates within unit 70 and does not exhibit apparent vertical offset (Fig. 6b). An additional event, C2, may be present but cannot be distinguished from the youngest event, C1. Event C2 is inferred because units 75 and 80 are offset with an apparent vertical sense of displacement (Fig. 6). The C1 event horizon is defined by faults that terminate within unit 100 (Fig. 6b). Expanded sections of the trench walls (Fig. 6) form the basis for descriptions of the event horizon stratigraphy and structure.

Event C4

On the northwest wall, event C4 horizon is defined by the top of unit 50. The top of unit 55 is subparallel to that of unit 50, so it is possible that the event horizon is at the top of unit 55, but it is not fractured except by what we infer to be event C3 (see following section). Event C4 offsets units 35, 40, 45, and 50 with a similar amount of apparent vertical separation and may have produced an upslope-facing scarp (Fig. 6a). Unit 55 may be a local colluvial wedge from the C4 event scarp. The vertical component is readily apparent in the offset paleosols of units 35 and 40, as well as within unit 45 on the southeast trench wall (Fig. 6b). On the south-

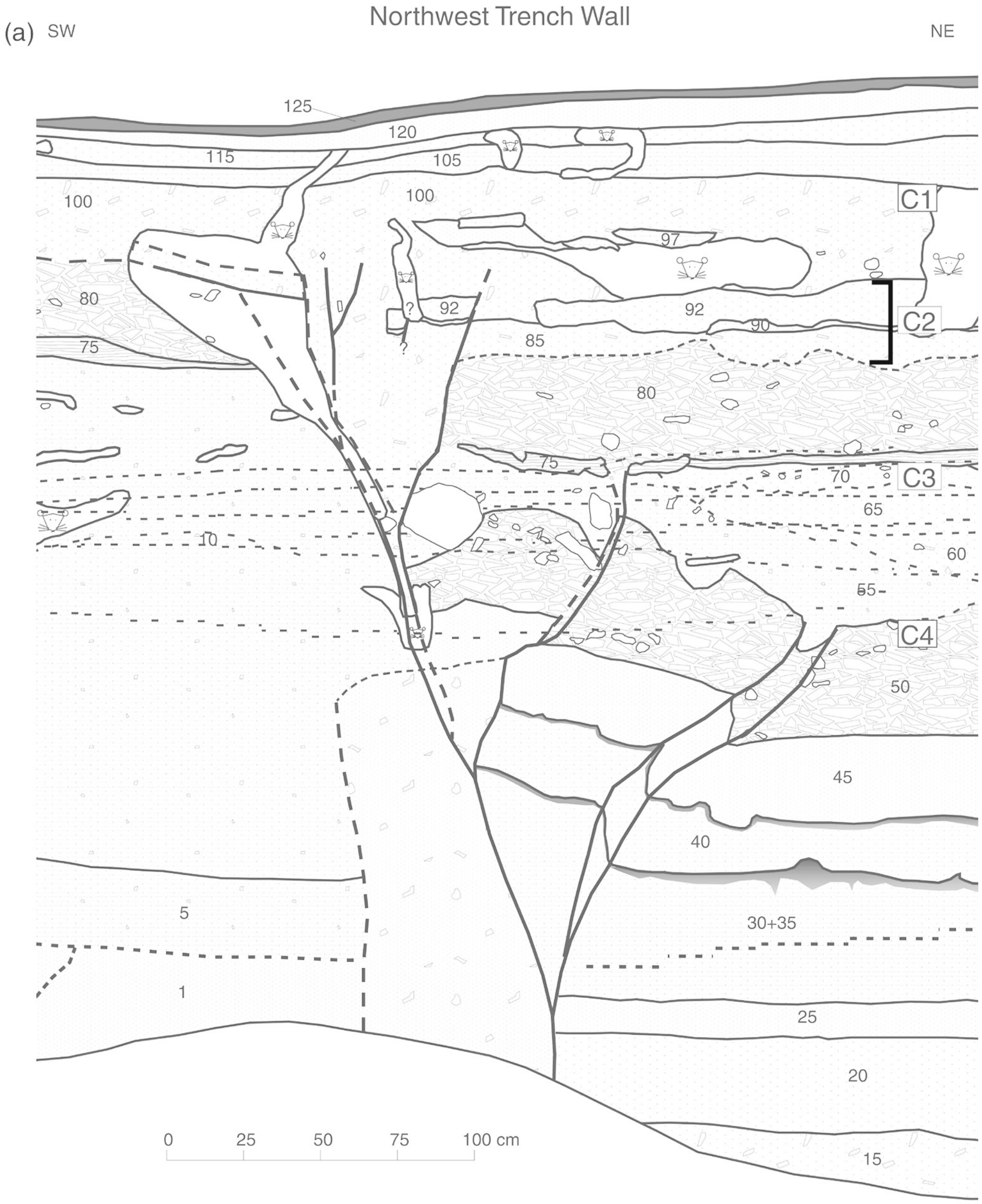

Figure 6. Enlarged version of the trench log (Fig. 5). Boxed labels indicate event horizons. (a) The northwest wall provides good evidence for event horizon C4, with apparent vertical offsets extending though unit 50, and event C3 extending up to unit 75. Event C2 is inferred by the apparent vertical offset of units 75 and 80. A large burrow in the main trace of event C1 prevents clear exposure of this event. (Continued on next page.)

east wall, event C4 created a small fissure with an apparent vertical sense of slip into which orange sand from unit 45 was incorporated (Fig. 6b, 7). The vertical component of slip is not seen in unit 50 on the southeast wall because unit 50 truncates against a younger fault strand. On the northwest trench wall, a small fissure filled with unit 55 lies along the same set of faults. If the fissures contain those materials exposed at the ground surface when they were open, the difference between the fissure contents across the trench indicates that units 45 and 55 were both on the ground surface at the time of rupture (unlikely), or that unit 45 was tectonically incorporated into the void within units 35–45 as evident on the southeast wall. Alternatively, the different fissure fills represent two earthquakes, but there is no other evidence preserved to differentiate two separate events.

Event C3

The C3 event horizon is best expressed on the southeast wall where the fault zone is 1 m wide and characterized by closely spaced fractures. All units below 75 apparently ter-

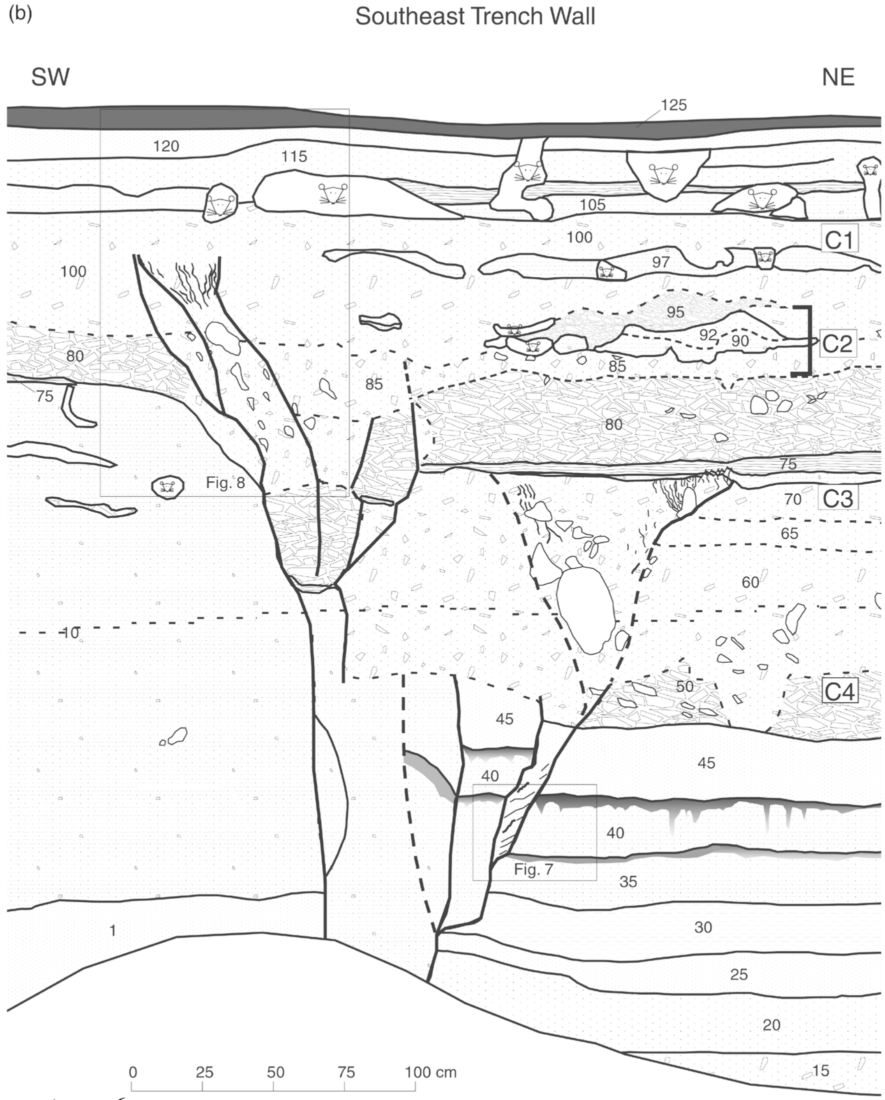

Figure 6. (b) The southeast wall provides better evidence for the C3 event from the extensive fractures present under unit 75. Fractures and subvertically aligned clasts attributed to event C1 are also better exposed on this wall. Event C4 is better exposed on the northwest wall. C2 is inferred on both walls by the vertical separation of units 75 and 80. The approximate coverage of Figures 7 and 8 are shown with the rectangles on Figure 6b.

minate against the fault (Fig. 6b). Enigmatic fractures extend partially into unit 75. We interpret the fractures as the product of compaction, creep (afterslip?), or settlement during shaking in younger earthquakes. A compaction or settlement origin is supported because the fine millimeter scale laminations of unit 75 are not offset. An alternate interpretation is that the C3 fractures may be associated with minor fault creep shortly after deposition of unit 75.

Event C3 appears to be a strike-slip event on a single trace with no topographic (vertical) offset because the overlying unit (75) is a thin, fine-grained unit and is found on both sides of the fault. If there had been a scarp at the time unit 75 was deposited, there should be some corresponding change in thickness across the fault. Additional traces may have moved during event C3 and may have subsequently been overprinted by displacement from younger earthquakes so that they are no longer distinguishable. However, the lack of observable vertical displacement suggests that C3 may have been a relatively minor displacement event on a single trace, possibly followed by a few millimeters of creep.

Event C2 or C1/C2

An event is defined by vertical separation of units 75 and 80 to form a paleoscarp approximately 0.4 m high. The event is labeled C2 in Figures 5 and 6 to distinguish it from a possibly younger event, C1. The evidence for interpreting each event is described separately, although it is important to note that they cannot be reliably distinguished and may represent a single rupture. Event C2 occurred sometime after unit 80 was deposited. Event C2 must have occurred prior

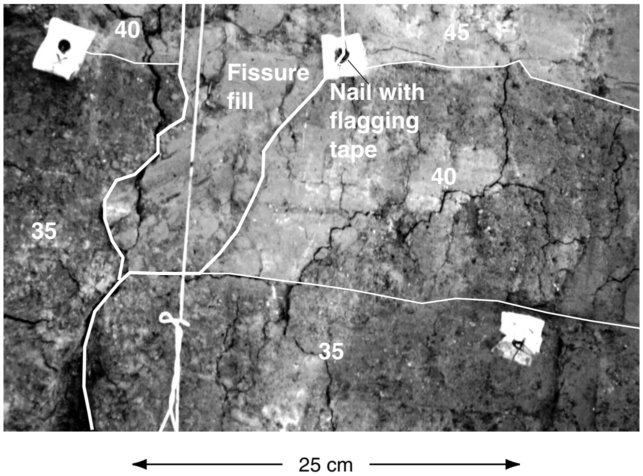

Figure 7. Photograph of a fissure on the southeast wall created during the C4 event. This rupture caused apparent vertical offset of units 35, 40, 45, and 50. Note fabric within the fissure dips 45° to the left. Nails, flagging, and string indicate the scale. See Figure 6b for location. Photo flipped to match orientation of trench logs (Figs. 5 and 6).

to deposition of the top of unit 100 because unit 100 is present on both sides of the fault zone and does not appear to be displaced vertically. The upper part of unit 100 does not appear to be faulted. As described in the section on fault zone stratigraphy, unit 80 is thinner on the southwest (upthrown) side of the fault, suggesting that it was eroded after occurrence of C2 and prior to deposition of unit 100. An alternative explanation for the difference in thickness is the natural variation in deposition of coarse channel gravels of unit 80.

Between units 80 and 100, the precise event horizon cannot be identified because the intermediate units 85–95 are poorly defined, bioturbated, discontinuous, and present only on the northeast side of the fault. Units 85–95 may have been deposited against a scarp on the northeast side of the fault after event C2 or they may be part of a channel sequence deposited at the same time as unit 80 or afterward. Their age cannot be determined relative to event C2. Unit 97 is interpreted as an infilled burrow that has been partially reoccupied. Therefore, the age of event C2 is only constrained by the requirement that it occurred after deposition of unit 80 and prior to deposition of the top of unit 100.

Event C1 or C1/C2

The youngest event horizon, C1, is defined by upward termination of fractures and vertically aligned clasts (Fig. 8) beneath unbroken beds (units 105–125). The stratigraphic level of event C1 is poorly constrained on the northwest wall of the trench because there are several burrows in and near the fault zone (Fig. 6a). There are some fractures and some discontinuous units to the northeast of the main fault trace (Fig. 6a). On the southeast wall, there are subvertically aligned clasts up to 7 cm long in the fault zone (Fig. 6b). Above the clasts is an area of closely spaced fractures (Fig. 8). These fractures terminate within unit 100. This does not preclude unit 100 from being the ground surface at the time of event C1. More than 70% fault strands in strike-slip ruptures do not reach the ground surface (Bonilla and Lienkaemper, 1990). Just above unit 100, the stratigraphy is approximately horizontal, suggesting that event C1 was strike slip and formed little or no scarp.

Event C2/C1

Another interpretation is that C1 and C2 are the same event, C1/C2. There are no distinct fault strands that terminate at a C2 event horizon. This could be explained by reactivation of C2 faults during event C1, or by C2 and C1 being the same event. A single earthquake could have caused two apparent events if units 75 and 80 dip to the northwest and the units above are horizontal beds. As described in the fault zone Stratigraphy section, unit 80 (and possibly overlying units) may be a channel deposit. Unit 80 has different thickness on either wall of the trench. It may have a fluvial gradient (primary dip) that is greater than the dip of most alluvial fan units exposed in the trench. In that case, strike-slip displacement could create apparent vertical displacement in the trench walls. However, blocks of units 75 and 80 appear to have fallen into a large (0.5 by 0.6 m) fissure (Fig. 6b), indicating there was at least an opening component during slip in event C2 (making a vertical component more reasonable). In addition, the local dip (as measured between the two trench walls) of the top of layer 75 is only 0.5° to the northwest. This gentle dip is consistent with the present-day topography of the site that slopes approximately 1° to the northwest. Such a dip would produce only a few cm of apparent offset for several meters of strike-slip displacement. Therefore, the evidence indicates that at least one event (C1/C2) occurred and that two separate events (C1 and C2) cannot be ruled out.

Age Constraints

Radiocarbon dates from two detrital charcoal samples and one bulk soil sample, in combination with pollen analysis and historical seismicity, provide constraints on event ages.

Radiocarbon Dating

Two charcoal samples from the paleosol capping unit 35 were accelerator mass spectrometer (AMS) dated to cal. A.D. 1058–1291 and cal. A.D. 1039–1281 (Table 1, Fig. 9). The paleosol contained abundant pieces of charcoal up to 0.3 cm in length, giving the paleosol a distinct, dark appearance. There are several possible explanations for the unusual abundance of charcoal in the paleosol. It might have been generated by an in situ burn or deposited as detrital charcoal by runoff following a wildfire. In either case, the

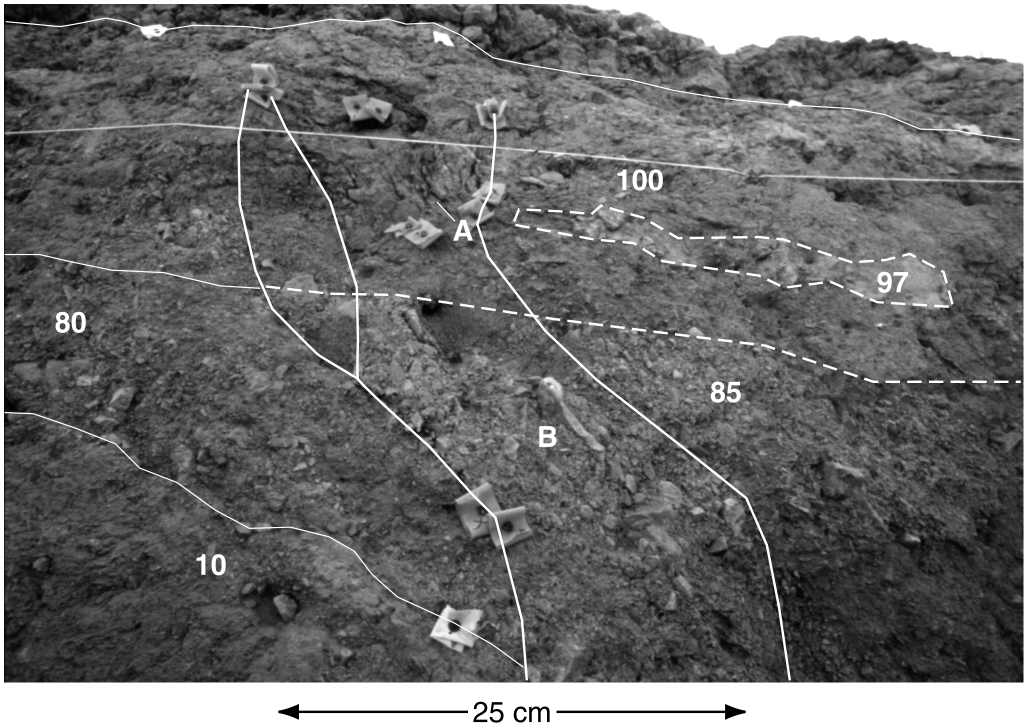

Figure 8. Photograph of the upper fault zone on the southeast wall. This photo was taken from the bottom of the trench so the view is oblique to the wall. Label A indicates vertical fractures that define the C1 event horizon. Label B indicates vertically aligned clasts that define the fault zone. Lines show the width of the zone with a vertical fabric developed during the C1 event. Nails, flagging, and string indicate the scale. See Figure 6b for location. Photo flipped to match trench logs (Figs. 5 and 6). Only the most distinct units are depicted.

Table 1
Radiocarbon Analysis for ^{14}C Samples*

Sample Number	Unit Sampled	Measured Radiocarbon Age†	$^{13}C/^{12}C$	2σ Calibrated Age Range	Material Type
LY4-99-2	35	810 ± 50 BP	−25‡	A.D. 1058–1291§,‖	charcoal fragment
LY4-99-5	35	840 ± 60 BP	−25‡	A.D. 1039–1281§,‖	charcoal fragment
LY4-99-31a	75	2680 ± 60 BP	−24.3	B.C. 995–765§,#	composite charcoal pieces from silt unit

*See Figure 9 for the probability distributions of LY4-99-2 and LY4-99-5.
†BP, years before A.D. 1950.
‡Assumed value.
§Calibrated using the University of Washington Quaternary Isotope lab Radicarbon Calibration program rev 4.3 (online at *http://depts.washington.edu/qil/calib/calib.html*); Stuiver *et al.*, (1998a, b).
‖AMS date from Lawrence Livermore National Laboratories
#AMS date from Beta Analytic

charcoal was subsequently incorporated into the paleosol, making the origin of the charcoal difficult to determine.

A composite radiocarbon date from a bulk sediment sample of unit 75 was analyzed to provide additional age control. This unit contained numerous small (<0.5 mm) pieces of detrital charcoal, so the organic matter was concentrated from the sediment, and a composite of this material was dated. The AMS conventional radiocarbon age determined for this sample was cal. 995–765 B.C. This sample is significantly older than both samples from unit 35, suggesting that the charcoal was reworked or had a significant inherited age.

Pollen Dating

Pollen can be introduced into sediment in three ways: (1) through a constant pollen rain at the surface of each unit when it was at the ground surface, (2) through pollen that rained onto the surface of the drainage basin and was incorporated into the flows deposited as units, and (3) through pollen that was introduced to buried sediment as water from the surface infiltrated the deposit. In our analysis, we assume pollen age represents the age of the paleosurface at the time of deposition of the unit, thus implying that infiltration transport of pollen is minimal. We collected bulk samples from fine grained units 70, 90, and 100. We cannot preclude infiltration into unit 100, however, the assumption that infiltration transport is insignificant is supported by our finding (described below) that introduced species are identified only in the uppermost sampled unit (unit 100).

We attempted two approaches that use pollen contained within the silt and silty matrix of units 70, 90, and 100. The first is to separate and directly radiocarbon date the pollen itself. Bulk sediment is processed to concentrate the pollen, which can then be manually separated to make sure there is no detrital charcoal in the sample before dating it (Davis, 1992). We concentrated the pollen from samples taken from locations shown on Figure 5. None of these units had pollen concentrations that would make this method practical (unit 70 had the highest concentration of 50,000 grains/cm^3).

The second method is to identify the pollen types in the units and look for exotic recently introduced species indicating historical ages. Four species that are common indicators of historical time periods were identified in unit 100. These are *eucalyptus*, *salsola* (Russian thistle or tumbleweed), *erodium* (storksbill), and *sporormiella* (spore of a dung fungi) (Table 2). All of these species were present in the top of unit 100 but they were not seen in units 90 or 70. The dates of exotic pollen species introduction define a maximum age for the upper part of unit 100, and a minimum age for units 70 and 90, assuming no percolation of pollen after deposition. Samples were collected from outside the fault zone in areas that were not visibly bioturbated to minimize the chance of contamination by percolation. The sample from unit 100 was collected 8 m to the northeast and slightly higher within the unit than the vertical fractures associated with the C1 event (Fig. 5). The location of the sample from unit 100 is suitable to assess the age of the unit if it is a single, massive unit. At the sample location, the lack of visible bioturbation or clear soil development suggests that unit 100 was at the ground surface for a relatively short time prior to burial. However, if unit 100 is bioturbated, then the age of the pollen may only represent the age of the top of the unit when it was at the ground surface and may postdate the youngest event. Therefore, the age of the pollen cannot be definitively related to the age of faulting.

As seen in Table 3, the two most recently introduced species identified in unit 100 are *salsola* and *eucalyptus*. The first *eucalyptus* trees were introduced in the early 1850s, and it takes approximately a decade for the pollen to be widely dispersed (Mudie and Byrne, 1980). Therefore, it is likely that the sample of unit 100 was deposited no earlier than 1860. Myron Angel wrote in 1883 that there was only one

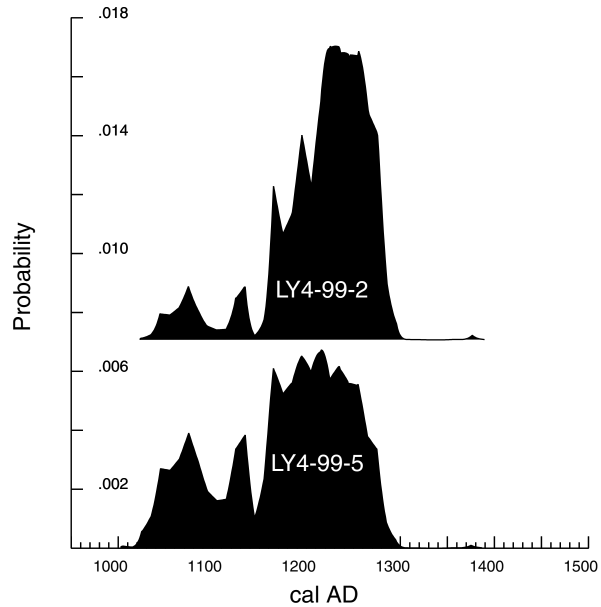

Figure 9. Probability distributions for calibrated ages of LY4-99-2 and LY-99-5 ^{14}C samples. Curves were computed using the University of Washington Quaternary Isotope lab Radicarbon Calibration program rev 4.3 (online at *http://depts.washington.edu/qil/calib/calib.html*) (Stuiver *et al.*, 1998a, b).

Table 2

Presence of Historic Pollen Present in Units 70, 90, and 100

Unit	*Eucalyptus*	*Salsola*	*Erodium*	*Sporormiella*	Total Pollen Concentration (grains/cm^3)
100	Y	Y	Y	Y	26,000
90	N	N	N	N	20,923
70	N	N	N	N	49,462

Pollen types observed by Pat Fall and Owen Davis during concentration determinations and analysis for suitability for radiocarbon dating. See Figure 5 for locations.

homestead in the Carrisa Plain near Painted Rock that did have *eucalyptus* trees growing around it (Angel, 1966). The Homestead Act of 1862 allowed people to claim quarter sections of land but required them to demonstrate that they were improving the property. A popular way to fulfill this requirement while also providing a windbreak was to plant *eucalyptus* trees. Therefore, the widespread planting of *eucalyptus* probably began in the 1860s, which would imply a unit that contained the pollen might date to 1870.

The *salsola* pollen was the most recently introduced of the historic pollen species identified in the upper part of unit 100 (Table 3). *Salsola*, or tumbleweed, was introduced from Russia in 1873 or 1874. It was accidentally shipped to South Dakota with flax seed. Tumbleweed spread quickly because the seeds are dispersed widely and it is drought resistant (Kirkpatrick, 1992). Because *salsola* pollen is present in the

Table 3
Introduction of Exotic Pollen Species in California

Pollen Species	Description	Date Introduced to California
Eucalyptus	Australian gum tree	A popular way to improve claim as required by the Homestead Act of 1862,* *eucalyptus* was first introduced to California in the early 1850s in the Bay Area.† Mudie and Byrne (1980) assigned a date of 1880 to the first appearance of *eucalyptus* pollen in Marin County (in the Bay Area). The first record of homesteads with *eucalyptus* in the Carrizo are from the 1860s.‡
Salsola	Tumbleweed/Russian thistle	Brought to the United States from Russia in 1873 or 1874 when it was accidentally included in a shipment of flax seed sent to South Dakota.§
Erodium	Storksbill	Introduced early to California, it was found in the adobe walls of Spanish missions established in 1776 and 1797.‖
Sporormiella	Dung spore	Usually indicates the presence of grazing animals;‖ cattle grazing occurred in the Carrizo in the 1850s and probably before that.‡

*J. Cooper, personal comm., 1999.
†Mudie and Byrne (1980).
‡Angel (1966).
§Kirkpatrick (1992).
‖Davis (1992).

upper layer of unit 100, this part of the unit must be younger than 1873.

Historical Ruptures

The historical record of earthquakes also provides some constraints on the age of the youngest event. The 1857 earthquake ruptured through the LY4 site because there are historical records confirming that it ruptured from Parkfield to just north of Cajon Pass (Sieh, 1978b). Therefore, events C2 or C1 or C1/C2 should have formed during the 1857 earthquake. There is no historic record of a surface rupture at the LY4 trench site after 1857. M $\sim$ 5.5 earthquakes occurred in the area in 1877 and 1908 (Toppozada *et al.*, 2000). However, the area is still very sparsely populated with restricted access for scientists, and historic records may be incomplete for seismic and/or creep events. Although the 1966 and 1934 Parkfield earthquakes ruptured only the Parkfield segment, we know very little about the earliest historical Parkfield events. Analyses of isoseismal data suggest that the 1901 and 1922 ruptures could not have been of a large enough magnitude to have ruptured into the Cholame segment (Bakun and Wentworth, 1997). However, there are almost no data for the 1881 Parkfield event, so we cannot preclude a rupture at the LY4 site from historical records alone.

Discussion

Recurrence Intervals

Our results above indicate that 3 or possibly 4 surface-rupturing earthquakes occurred at the LY4 site since deposition of the detrital charcoal LY4-99-2 dated at 1058–1291 cal. A.D. One way to compare the rupture potential of the Cholame segment (at the LY4 site) with other portions of the San Andreas fault is to calculate the average recurrence interval for each site through 2000. This method is unbiased because it does not require correlation of ruptures between sites. Table 4 shows the reported events for major paleoseismic sites along the southern SAF, the number of ruptures, maximum age (2σ), and average recurrence intervals. Interestingly, assuming the maximum number of recognized ruptures at the LY4 site (C1–C4) and no missing ruptures, the Cholame segment appears to have one of the longest recurrence intervals, nearly twice as long as Pallet Creek. This finding is inconsistent with the hypothesis that the Cholame segment ruptures frequently with relatively smaller magnitudes, as proposed by Sieh and Jahns (1984), Harris and Archuleta (1988), WGCEP (1988), and Arrowsmith *et al.*, (1997) and the geologically constrained calculations of Ward (1996).

These studies have assumed the Cholame segment (with 3- to 6-m geomorphic offsets) should rupture both during large Carrizo segment events with offsets of 7–9 m (such as in 1857), and on its own with lower slip to catch up to the Carrizo segment and maintain a uniform slip rate. According

Table 4
Average Recurrence Intervals through A.D. 2000 for Sites along the Southern San Andreas Fault

Paleoseismic Site	Number of Ruptures	Maximum Age (2σ) of Oldest Rupture (cal. A.D.)	Average Recurrence (yr)
Cholame	4	1058	236
Bidart Fan*	5	1218	156
Mill Potrero†	3	1450	183
Pallett Creek†	10	700	130
Wrightwood‡	11	400	146
Indio†	4	1050	238

*Grant and Sieh (1994).
†WGCEP (1988).
‡Fumal *et al.* (1993); Weldon (1991).

to this hypothesis, the average recurrence interval for earthquakes on the Cholame segment should be shorter than in the Carrizo. Arrowsmith *et al.* (1997) explored the possible rupture scenarios of catch-up earthquakes and their resulting magnitudes. Because the southern end of the Cholame segment is poorly defined, they presented several scenarios for varying rupture lengths and their maximum moment magnitudes. These include a Parkfield event (M 6.5; length = 35 km), a Parkfield to Bitterwater Valley rupture (M 6.8; length = 62 km), a Parkfield to Bidart Fan event (M 7.1; length = 108 km), and a Cholame to Bidart Fan event (M 7.0; length = 73 km) (Fig. 1). Our work at the LY4 site suggests that there have been fewer events along the Cholame segment than in the Carrizo, implying that the proposed rupture scenarios may occur infrequently. However, paleoseismic data sets often contain the minimum number of ruptures because there is the possibility of unrecognized earthquakes that are not preserved at a site. If events were missed in this trench site, or the radiocarbon samples had inherited age, then the recurrence interval for Cholame would be closer to that expected by WGCEP (1988).

Implications for Rupture Potential and Size of Events

The relative size of events C1–C4 may be roughly estimated from the amount of apparent displacement and correlation with rupture events at other sites. It appears that two events, C2 and C4, produced topographic changes in the form of uphill-facing scarps (Fig. 5). The 1857 earthquake generated significant surface faulting in the area, so it is likely that the apparent scarp of event C2 or C2/C1 represents a large earthquake. Therefore, event C4 may also have been a large earthquake because it generated a comparable size scarp. If event C1 represents a distinct earthquake, then it appears that two events, C1 and C3, were generated by relatively minor faulting with little or no vertical separation. This interpretation weakly suggests that both large (e.g., 1857) and smaller magnitude ruptures have occurred at the site, in alternating pattern.

Alternatively, if the Cholame segment only ruptures during Carrizo events, and the Carrizo record at the Bidart site is an accurate record of earthquake recurrence, then the Cholame–Carrizo offsets from the 1857 earthquake cannot be typical or there would be a slip deficit in the Cholame segment. If there are individual Cholame or Parkfield–Cholame events, then some of the Carrizo ruptures did not also rupture the Cholame and Parkfield segments. This implies that the length of the Carrizo events would be shorter than the 1857 rupture. This was not expected by previous studies (e.g., Schwartz and Coppersmith, 1984; Sieh and Jahns, 1984), which implied the Carrizo will always rupture in larger earthquakes with adjacent segments. This is also assumed in the synthetic seismicity models of Ward (1996). The Carrizo ruptures generated by these models always rupture the Cholame segment (although the southern end of these ruptures is more variable) while allowing for Parkfield–Cholame ruptures.

Conclusions

Based on our analysis of the LY4 excavation, the central Cholame segment has experienced at least three and possibly four ruptures since cal. A.D. 1039–1291. The dates of individual events are poorly constrained, and there is uncertainty in identifying the 1857 rupture horizon. Despite these limitations, the rupture history provides insights on the behavior and rupture potential of the Cholame segment. Two events (C4 and C2 or C2/C1) were major strike-slip surface ruptures with tens of centimeters of apparent vertical offset. Events C3 and possibly C1 may have been smaller and were not associated with more than a few cm of vertical offset. Analysis of pollen species present in the stratigraphy suggests that the most recent earthquake occurred within a few decades of 1873 or 1874. The youngest event may have been the 1857 Fort Tejon earthquake. Although unlikely, we cannot rule out the possibility of post-1857 displacement. If none or few earthquakes are missing from the paleoseismic record at this site, there appear to be fewer earthquakes in this area than expected by conventional models of earthquake hazard (Sieh, 1978b; WGCEP, 1988; Harris and Archuleta, 1988; Ward, 1996, Arrowsmith *et al.*, 1997).

Acknowledgments

Many thanks are due to Darrell Twisselman for allowing us access to his property and permission to excavate there. D. Rhodes made significant contributions in the early phase of the project. Thanks to L. Amoroso, J. D'Andrea, K. Fergason, G. Hilley, S. Holloway, M. Nowicki, S. Nowicki, S. Robinson, M. Taylor, Z. Washburn, and E. Young for help in the field and to M. Ballie for help in the lab. T. Fumal, H. Stenner, T. Dawson, D. Schwartz, T. Rockwell, J. Young, and M. Robertson engaged us in useful discussions at the trench site. D. Schwartz, T. Rockwell, T. Dawson, and T. Fumal provided constructive reviews of the manuscript. P. Fall, G. Seitz, S. Cunha, and O. Davis provided valuable insight into the potential use of pollen for constraining rupture ages. J. Cooper provided us with historical information on the development of the Carrizo Plain area. This research was supported by the Southern California Earthquake Center (SCEC). SCEC is funded by NSF Cooperative Agreement EAR-8920136 and U.S. Geological Survey Cooperative Agreements 14-08-0001-A0899 and 1434-HQ-97AG01718. The SCEC Contribution No. for this article is 495.

References

Angel, M. (Editor) (1966). *Reproduction of Thompson and West's History of San Luis Obispo County, California with Illustrations and Biographical Sketches of Its Prominent Men and Pioneers [1883]*, Howell-North Books, Berkeley, California, 391 pp.

Arrowsmith, R., K. McNally, and J. Davis (1997). Potential for earthquake rupture and M7 earthquakes along the Parkfield, Cholame, and Carrizo segments of the San Andreas Fault, *Seism. Res. Lett.* **68,** 902–916.

Bakun, W. H., and A. G. Lindh (1985). The Parkfield, California, earthquake prediction experiment, *Science* **229,** 619–624.

Bakun, W. H., and C. M. Wentworth (1997). Estimating earthquake location and magnitude from seismic intensity data, *Bull. Seism. Soc. Am.* **87,** 1502–1521.

Bonilla, M. B., and J. J. Lienkaemper (1990). Visibility of fault strands in exploratory trenches and timing of rupture events, *Geology* **18,** 153–156.

Davis, O. K. (1992). Rapid climatic change in coastal southern California inferred from pollen analysis of San Joaquin marsh, *Quaternary Res.* **37,** 89–100.

Dibblee, T. W. Jr. (1973). Regional geologic map of San Andreas and related faults in Carrizo Plain, Temblor, Caliente, and La Panza ranges and vicinity, California, U.S. Geol. Surv. Misc. Invest. Map I-0757, scale 1:125,000.

Fumal, T. E., S. K. Pezzopane, R. J. Weldon II, and D. P. Schwartz (1993). A 100-year average recurrence-interval for the San Andreas fault at Wrightwood, California, *Science* **259,** 973.

Graf, W. L. (1988). *Fluvial Processes in Dryland Rivers*, Springer-Verlag, Berlin.

Grant, L. B. (1993). Characterization of large earthquakes on the San Andreas fault in the Carrizo Plain: implications for fault mechanics and seismic hazard, *Ph.D. Dissertation*, California Institute of Technology, Pasadena, California.

Grant, L. B. (1996). Uncharacteristic earthquakes on the San Andreas fault, *Science* **272,** 826–827.

Grant, L. B., and K. Sieh (1994). Paleoseismic evidence of clustered earthquakes on the San Andreas fault in the Carrizo Plain, California, *J. Geophys. Res.* **99,** 6819–6841.

Harris, R. A., and R. J. Archuleta (1988). Slip budget and potential for a M7 earthquake in central California, *Geophys. Res. Lett.* **15,** 1215–1218.

Jennings, C. W., R. G. Strand, and T. H. Rogers (1977). Geologic map of California, Calif. Div. Mines Geol. Sacramento, California, Scale 1:750,000.

Kirkpatrick, Z. M. (1992). *Wildflowers of the Western Plains: A Field Guide*, University of Texas Press, Austin, Texas, 240 pp.

Lienkaempaer, J. J. (2001). 1857 slip on the San Andreas fault southeast of Cholame, California, *Bull. Seism. Soc. Am.* **91,** no. 6, 1659–1672.

Lienkaemper, J. J., and T. A. Sturm (1989). Reconstruction of a channel offset in 1857(?) by the San Andreas Fault near Cholame, California, *Bull. Seism. Soc. Am.* **79,** 901–909.

Mudie, P. J., and R. Byrne (1980). Pollen evidence for historic sedimentation rates in California coastal marshes, Est. Coastal Mar. Sci. **10,** 305–316.

Schwartz, D. P. and K. J. Coppersmith (1984). Fault behavior and characteristic earthquakes: examples from the Wasatch and San Andreas fault zones, *J. Geophys. Res. B* **89,** 5681–5698.

Sieh, K. E. (1978a). Slip along the San Andreas fault associated with the great 1857 earthquake, *Bull. Seism. Soc. Am.* **68,** 1421–1448.

Sieh, K. E., and R. H. Jahns (1984). Holocene activity of the San Andreas fault at Wallace Creek, California, *Geol. Soc. Am. Bull.* **95,** 883–896.

Sims, J. D. (1987). Late Holocene slip rate along the San Andreas fault in southern California, Geological Society of America Abstracts with Programs, Vol. 19, 451.

Southern California Earthquake Center Working Group (SCECWG) on the Probabilities of Future Large Earthquakes in Southern California (1994). Seismic hazards in southern California: probable earthquakes, 1994–2024, *Bull. Seism. Soc. Am.* **85,** 379–439.

Stone, E. M. (1999). Geomorphology, structure and paleoseismology of the central Cholame segment, Carrizo Plain, California, M.S. Thesis, Arizona State University, Tempe, Arizona, 100 pp.

Stuiver, M., and T. F. Braziunas (1993) *The Holocene* **3,** 289–305.

Stuiver, M., P. J. Reimer, E. Bard, J. W. Beck, G. S. Burr, K. A. Hughen, B. Kromer, F. G. McCormac, J. v.d. Plicht, and M. Spurk, (1998a) Radiocarbon 40:1041–1083.

Stuiver, M., P. J. Reimer, and T. F. Braziunas (1998b) Radiocarbon 40:1127–1151. (revised dataset).

Toppozada, T., D. Branum, M. Petersen, C. Hallstrom, and M. Reichle (2000). Epicenters of and areas damaged by $M \geq 5.5$ California earthquakes, 1800–1999, California Division of Mines and Geology, Map Sheet 49, scale 1:5,000,000.

Wallace, R. E. (1991). Ground-squirrel mounds and patterned ground along the San Andreas fault in central California, *U.S. Geol. Surv. Open-File Rept. 91-149*, 21 pp.

Ward, S. N. (1996). A synthetic seismicity model for southern California: Cycles, probabilities, and hazard, Journal of Geophysical Research. 101, 22393–22418.

Weldon, R. J. II (1991). Active tectonic studies in the United States in 1987–1990, *Rev. Geophys.* **29,** 890–906.

Working Group on California Earthquake Probabilities (WGCEP) (1988). Probabilities of large earthquakes occurring in California on the San Andreas Fault, *U.S. Geol. Surv. Open-File Rept. 88-398*, 62 pp.

Department of Geological Sciences
Arizona State University
Tempe, Arizona 85287-1404
(E.M.S., J R.A.)

Department of Environmental Analysis and Design
University of California
Irvine, California 92697-7070
(L.B.G.)

Manuscript received 11 January 2000.